

## Article

# Simultaneous Removal of Metal Ions from Wastewater by a Greener Approach

Lubna A. Ibrahim <sup>1,2,\*</sup>, Marwa E. El-Sesy <sup>2</sup>, ElSayed ElBastamy ElSayed <sup>2</sup>, Martina Zelenakova <sup>3,\*</sup>,  
Maria Hlinkova <sup>4</sup>, Essam Sh. Mohamed <sup>5</sup> and Mohamed Abu-Hashim <sup>6</sup>

- <sup>1</sup> Water Management Research Institute (WMRI), National Water Research Center (NWRC), El-Qanater El-Khairia 13621, Egypt
- <sup>2</sup> Central Laboratory for Environmental Quality Monitoring, National Water Research Center (NWRC), El-Qanater El-Khairia 13621, Egypt
- <sup>3</sup> Department of Environmental Engineering, Faculty of Civil Engineering, Technical University of Kosice, 04200 Kosice, Slovakia
- <sup>4</sup> Faculty of Civil Engineering, Institute of Technology, Economics and Management in Construction, Technical University of Kosice, 04200 Kosice, Slovakia
- <sup>5</sup> Institute of Global Health and Human Ecology, The American University in Cairo, New Cairo 11835, Egypt
- <sup>6</sup> Soil Science Department, Faculty of Agriculture, Zagazig University, Zagazig 44511, Egypt
- \* Correspondence: lubnaibrahim43@gmail.com (L.A.I.); martina.zelenakova@tuke.sk (M.Z.)

**Abstract:** The examination of the performance of raw and immobilized *S. (Saccharomyces) cerevisiae* in the simultaneous abatement of metal ions from wastewater effluent is the focal point of this article. The optimal storage time for raw and immobilized *S. cerevisiae*, during which they can be utilized, was estimated. The outcomes revealed that as the initial metal ion concentrations increased, the adsorption capacity improved, while the removal efficiency of *S. cerevisiae* yeast cells decreased, with the highest uptake obtained at the optimal conditions: pH = 5.0, 2.0 g *S. cerevisiae*/L, 25 °C, and a contact time of 25 min. The maximum adsorption capacities ( $q_{\max}$ ) for Pb(II), Cd(II), and Ni(II) ions are shown by Langmuir at 65, 90, and 51 mg/g, respectively. It was discovered that the metal ions' biosorption reactions were spontaneous and were fitted by the pseudo-second-order model. The mechanisms of the metal ions' abatement were explained by using XRD (X-ray diffraction), FTIR (Fourier transform infrared spectroscopy), (BET) Brunauer–Emmett–Teller, and TEM (transmission electron microscopy) outputs. EDTA and citric acid can eliminate more than  $70 \pm 4$  and  $90 \pm 5\%$  of the adsorbed ions, respectively. The experiment of storage demonstrated that the immobilized *S. cerevisiae* was more stable for 8 months than the raw yeast.

**Keywords:** fixed-bed column; immobilized *S. cerevisiae*; industrial wastewater treatment



**Citation:** Ibrahim, L.A.; El-Sesy, M.E.; ElSayed, E.E.; Zelenakova, M.; Hlinkova, M.; Mohamed, E.S.; Abu-Hashim, M. Simultaneous Removal of Metal Ions from Wastewater by a Greener Approach. *Water* **2022**, *14*, 4049. <https://doi.org/10.3390/w14244049>

Academic Editor: Saglara S. Mandzhieva

Received: 31 October 2022

Accepted: 5 December 2022

Published: 12 December 2022

**Publisher's Note:** MDPI stays neutral with regard to jurisdictional claims in published maps and institutional affiliations.



**Copyright:** © 2022 by the authors. Licensee MDPI, Basel, Switzerland. This article is an open access article distributed under the terms and conditions of the Creative Commons Attribution (CC BY) license (<https://creativecommons.org/licenses/by/4.0/>).

## 1. Introduction

Climate change requires sustainable and innovative treatment approaches to deal with the quickly depleting water resources that have rendered water a competitive resource for many regions globally. Producing stable materials through low-cost approaches to provide adequate amounts of freshwater is the need of the water industry that has motivated many scientists and researchers to research nontraditional water treatment techniques to increase the quantity of water. Fast urbanization and industrialization in the world have prompted the introduction of heavy metals by industrial and mining activities: manure, paints, battery manufacture, and spillage of industrial wastes, plus pesticide-based metals [1]. Among the metal ions, lead (Pb(II)), cadmium (Cd(II)), and nickel (Ni(II)) ions are perceived to be huge ecological pollutants [2].

Several physicochemical treatment methods (precipitation, coagulation–flocculation, membrane processes, chemical precipitation, ion exchange, electrodeposition, and electrochemical techniques) have demonstrated adequate performance in the abatement of trace

elements from aqueous solutions [3–6] but remain economically nonviable because of the additional capital, unpredictable efficiency, generation of toxic sludge, high energy and reagent requirements, and high operational costs that have diminished their possibilities for widespread use [7,8]. Electrodeposition, as opposed to adsorption and chemical precipitation, is a more cost-effective and safe method of removing and recovering heavy metals from wastewater that does not require the utilization of chemicals [9,10]. Adsorption, in any case, remains a feasible alternative, particularly in developing nations, since it is environmentally benign, simple, inexpensive, and does not produce large sludge quantities [11,12]. In recent decades, various natural and manufactured adsorbents have been examined for their ability to eliminate heavy metals from contaminated solutions [13–20]; however, separating these adsorbents from the aqueous solution entails a complex process with additional costs, and structure stability should be emphasized [20].

Biosorption is a significantly more proficient strategy for the elimination of numerous pollutants, which include heavy metals, because of the accessibility of a diverse range of biosorbents that have low prices and adapt to various circumstances [21–24]. In this way, different sorts of microorganisms (bacteria, yeasts, algae, fungi) [25–27] have affirmed that they can recover heavy metals from aqueous solutions via biosorption [7,27–29]. *Saccharomyces cerevisiae* (*S. cerevisiae*) yeast is generally utilized in food biotechnology processes, such as the production of wine, bread, and beer. It is an especially appropriate organism for biological examinations and it has “generally regarded as safe (GRAS) status” [30]. Thus, efficient and low-cost processes for producing large-scale yeast biomass have evolved. *S. cerevisiae* is a promising biosorbent that has been shown to eliminate pesticides [31], mycotoxins [32], and trace elements from synthesized water or aqueous solutions, even when deactivated, and it has its highest efficiency in short contact times [7,29,33–45]. Furthermore, the encapsulation of *S. cerevisiae* in a biopolymer, for example, alginate [32,43,46–50], is an alternative strategy for their application, as well as being steadier, simple-to-deal with, and economical.

Hence, in this examination, the performance of *S. cerevisiae* (grown on Yeast Peptone Dextrose (YPD)) biomass at 25 °C for ions being rid from the water was assessed. The influence of pH, *S. cerevisiae* dose, initial metal ion concentration in solution, contact time, and temperature on ion biosorption efficiency and biosorption capacity of the biomass was examined. The equilibrium data have also been examined via isotherm, kinetic, and thermodynamic investigations. The biosorption mechanism of *S. cerevisiae* was explained by considering the XRD, FTIR, BET, and TEM techniques. The adequacy of different eluents (H<sub>2</sub>O, NH<sub>4</sub>NO<sub>3</sub>, EDTA-Na<sub>2</sub>, and citric acid) to desorb or regenerate the biosorbed metal ions was also examined. At last, the efficacy of *S. cerevisiae* and the fixed-based column (immobilized *S. cerevisiae*) for the abatement of metal ions from wastewater were compared and the best storage time after which they could be reused was determined. Outcomes verified the capacity of *S. cerevisiae* in the biosorption of mono-components from synthesized water and comparison of two approaches for the take-up of metal ions from real wastewater samples. The outcome of this investigation would be to provide eco-friendly metal ion abatement materials, stable for 8 months (m), mostly from wastewater of different multi-components.

## 2. Experimental

### 2.1. Wastewater Sampling

Screw-capped sterilized bottles were utilized for the collection of wastewater samples from “Al-Monairy for corn products, Madinat al-Āshir min Ramadān, As Sharqia, Egypt”. The fundamental products of that factory are corn (starch, flour, and grits), glucose, fructose, gluten (corn and feed), high maltose, dextrose, and maize oil that are widely used in most other manufacturing industries (i.e., pharmaceuticals, textile, paper, food products and feed). The color of gathered samples was black and specified by their high content of solids.

## 2.2. Reagent, Biosorbent, Media, Culture Condition, and Drying Process

All chemicals and supplements were of high-purity analytical grade. For aqueous solution preparation and cleaning purposes, double-deionized water (DDW) was utilized. Calcium chloride (95+%  $\text{CaCl}_2$ ) was purchased from Chem-Lab NV (made in Belgium), while sodium alginate (91–106%  $\text{C}_8\text{H}_7\text{O}_8\text{Na}$ ) was a Techno PharmChem product. YPD Broth was Merck (KGaA—Bioz) product. Ammonium nitrate (>99%,  $\text{NH}_4\text{NO}_3$ ), citric acid (>99%,  $[\text{HOC}(\text{COOH})(\text{CH}_2\text{COOH})_2]$ ), and Ethylenediaminetetraacetic acid disodium salt solution (0.5 M EDTA- $\text{Na}_2$  in  $\text{H}_2\text{O}$ ) were purchased from Sigma-Aldrich. *S. cerevisiae* culture was acquired from the Microbial products lab of the “National Research Center (NRC)/Egypt”.

Then *S. cerevisiae* was cultured on sterilized Yeast Peptone Dextrose (YPD) agar broth at  $25 \pm 1$  °C and then kept up at 4 °C on YPD agar slant. The media was prepared to comprise (w/v %): glucose, 2%; yeast extract, 1%; peptone, 2%, and agar, 2%. Each strain was cultured at  $25 \pm 1$  °C for 24 h at 150 rpm in sterilized media (YPD) and the cells were collected for that investigation. Strains were kept at  $-4 \pm 1$  °C until they were utilized in the trials [46,47]. After culturing, *S. cerevisiae* yeast cells were harvested by centrifugation at 6000 rpm for nine min. The harvest cells were rinsed with DDW few times to eliminate excess growth medium before being centrifuged. The *S. cerevisiae* yeast was dried in an autoclave at  $25 \pm 1$  °C until constant weight, homogenized, and saved in a desiccator until use.

## 2.3. Biosorption Parameters Investigation

For each investigated metal ion, all the examinations were performed by suspending the biosorbent in solution by varying the parameters: pH (2–8), ion concentration (25–250 mg/L), biosorbent dose (2–16 g/L), contact time (6–180 min), and temperature (15–40 °C), while the others stayed constant. The solution was incubated at 20 °C on a rotary shaker (150 rpm) for 2 h. The filtrate was centrifuged at  $6000 \times g$  for nine min and then filtered utilizing 0.45  $\mu\text{m}$  pore size filter paper to eliminate particle intrusion into the analytical equipment. The initial ( $C_i$ ) and equilibrium final ( $C_e$ ) concentrations of investigated metal ions were quantified (mg/L). Each trial had three repetitions, the results were averaged, and the standard deviation (STD) was calculated. The removal efficiency (RE%) and the adsorption capacity ( $q_e$ , mg/g) were estimated by Equations (1) and (2), in which  $V$  is the volume (L) of the solution, and  $W$  is the mass (g) of biosorbent [18,51].

$$\text{Removal Efficiency (RE\%)} = \frac{C_i - C_e}{C_i} \times 100 \quad (1)$$

$$q_e = (C_i - C_e) \frac{V}{W} \quad (2)$$

## 2.4. Laboratory Water Analyses

All examinations were conducted in an ISO 17025: 2017 certified laboratory of the “Central Laboratory for Environmental Quality Monitoring (CLEQM)”. The samples were subjected quickly to physical and chemical examinations as demonstrated by the Standard Methods for the Examination of Water and Wastewater [52]. The pH, electric conductivity (EC), and dissolved oxygen (DO) were estimated at 25 °C utilizing a pH meter InoLab WTW, conductivity meter InoLab, and DO meter, respectively. Trace metals and cations were estimated utilizing the ICP-MS, PerkinElmer product model SCIEX Elan 9000. Recovery studies for the investigated metal ions analyzed utilizing ICP-MS ranged from 98 to 102%.

## 2.5. Biosorption Isotherm, Kinetics, and Thermodynamics Studies

Two isotherm models (Langmuir and Freundlich), three kinetics models (pseudo-first-order (1st), pseudo-second-order (2nd), and intraparticle diffusion), and thermodynamic parameters were utilized to model the empirical data using the mathematical formulas [29,34,47]

prescribed in Table 1. The best isotherm and kinetics models were selected relying on the regression coefficients ( $R^2$ ), estimated statistically.

**Table 1.** Mathematical equations of both isotherm and kinetic models, and thermodynamics parameters utilized for the empirical data analysis.

	Model	Equation	Notations
Isotherm models	Langmuir	$\frac{C_e}{q_e} = \frac{1}{q_{\max}} K_d + \frac{C_e}{q_{\max}}$	where $C_e$ is the equilibrium (final) metal ions concentration (mg/L), $K_d$ is an apparent dissociation constant, $n$ indicates the intensity of the process, $q_{\max}$ represents the capacity for metal ion uptake when the surface is completely covered with metal ions, $K_f$ is a biosorption equilibrium constant, $q_e$ and $q_t$ (mg/g) are the amounts of Cd(II), Pb(II), and Ni(II) ions adsorbed on the adsorbent at equilibrium and time $t$ (min), respectively. $I$ is the intercept and $k_1$ (1/min), $k_2$ (g/mg min), $v_1$ (g/mg min), and $K_d$ (mg/g min <sup>0.5</sup> ) are the rate constant of pseudo-1st-order, pseudo-2nd-order, initial sorption rate, and intraparticle diffusion, respectively.
	Freundlich	$\ln q_e = \ln K_f + \frac{1}{n} \ln C_e$	
Kinetic models	Pseudo-first (1st)-order	$\log(q_e - q_t) = \log q_e - \left(\frac{k_1}{2.303}\right) \cdot t$	
	Pseudo-second (2nd)-order	$\frac{t}{q_t} = \frac{1}{v_1} + \frac{t}{q_e}$ $v_1 = k_2 q_e^2$	
	Intraparticle diffusion	$q_t = K_d t^{0.5} + I$	
Thermodynamic	Thermodynamic parameters	$-\Delta G^0 = -RT \ln K_D$ $\ln K = \frac{\Delta H^0}{RT} + \frac{\Delta S^0}{R}$ $\Delta G^0 = \Delta H^0 - T\Delta S^0$	$\Delta G^0$ , $\Delta H^0$ , and $\Delta S^0$ are the free energy change, enthalpy changes, and entropy change, respectively. $R$ (8.314 J/mol K) is the universal gas constant, $T$ is the absolute temperature (K), and $K$ is the equilibrium constant.

## 2.6. Characterization Techniques

X-ray diffraction patterns (XRD) of powder samples of *S. cerevisiae* and Pb(II)-biosorbed *S. cerevisiae* biomass were registered in a Broker D8 Advanced target Cuk $\alpha$  powder diffractometer ( $\lambda = 1.5418 \text{ \AA}$ ) over the range of  $2\theta = 0\text{--}80^\circ$  scale. FTIR for *S. cerevisiae* and uploaded Pb(II) was examined in KBr discs containing about 3% ( $w/w$ ) of finely ground powder of each sample using spectrophotometer PerkinElmer FTIR 1650 in El-Zagazig University. For treated *S. cerevisiae* and uploaded Pb(II): the surface area analysis, average particle size, and total pore volume were obtained by utilizing the Brunauer–Emmett–Teller (BET, HitachiVP-SEM S-3400N, Germany) method. The TEM for *S. cerevisiae* and uploaded Pb(II) was performed utilizing JEOL TEM-1400 electron microscope and optronics AMT CCD camera with 1632 pixel format as side mount configuration relying on the strategies applied by El-Sayed [48].

## 2.7. Yeast Cell Immobilization and Its Application for Simultaneous Treatment of Wastewater

The immobilization procedures were carried out in accordance with the procedure reported in Araujo et al. [49] (Figure 1). For biosorption fixed-bed column, a glass column (height 2.5 cm, inner diameter 0.38 cm) was packed with 2 g of calcium alginate beads loaded with *S. cerevisiae* [49,50]. During the treatment, the column temperature was kept constant at 25 °C. One liter (L) of the sample (pH 5.0) was pumped through the column at 1.5 mL/min for 25 min contact time. After a resident time, the samples were gathered and analyzed immediately as described before.



**Figure 1.** Immobilized *S. cerevisiae*.

### 2.8. Desorption Experiments from Loaded Cell Biosorbent

Desorption of Cd(II), nickel (Ni(II)), and lead (Pb(II)) from previously loaded resting immobilized cells was examined by utilizing deionized water (H<sub>2</sub>O), 1.0 mol/L of NH<sub>4</sub>NO<sub>3</sub>, 0.1 mol/L of EDTA-Na<sub>2</sub>, and 10% citric acid as eluents. The trials were tested with 0.036 g Cd(II)-, 0.034 g nickel (Ni(II)-, and 0.046 g lead (Pb(II))-loaded 1 g immobilized cell biosorbent in 50 mL plastic tubes containing 20 mL of each eluent. After 30 min of shaking at 25 °C, supernatants were centrifuged and analyzed for metal ions by ICP-MS. Adsorption capacities for each of the recently mentioned eluents were assessed by the amount of metal ion concentrations in the desorption solution. Sequential sorption–desorption cycles were repeated thrice trials to lay out the reutilizing of the adsorbent. In the meantime, biosorption capacity was also assessed.

### 2.9. Storage of the Yeast Cells

The free and immobilized *S. cerevisiae* was kept in a refrigerator at  $4 \pm 1$  °C in saline solution for 0 months (m), 2 m, 4 m, and 8 m, and then utilized for treating the collected wastewater samples.

### 2.10. Statistical Analyses

Data were exposed to investigation utilizing statistical software IBM® SPSS®, V 26, 2019, and reported as min, max, mean values, and standard deviation (SD). The statistical programs SPSS and Costat (V. 6.400, USA) were utilized to recognize and compare treatments utilizing analysis of variance (ANOVA) and multiple component tests.

## 3. Results and Discussion

### 3.1. Optimum Conditions and Modeling Biosorption Processes by *S. cerevisiae*

#### 3.1.1. Impact of pH on Biosorption Capacity

pH is the most critical consideration in the biosorption process. It impacts the competition of metal ions and the activity of the biomass functional groups [29,53]. The adsorption of different metal ions on *S. cerevisiae* was examined at pH values of 2, 3, 4, 5, 6, 7, and 8 to optimize the progression of the Cd(II), Pb(II), and Ni(II) removal rates with pH as shown in Figure 2A. The sorption capacity of the ions increases as the pH of the aqueous solution rises from 2 to 5 due to the protons preferentially binding to the superficial functional groups [29]. Then the capacity decreases as pH rises from 6 to 8 because of the  $-\text{OH}^-$  group competing with the binding sites on the *S. cerevisiae* cell wall to combine with metal ions and precipitate as metal complexes Cd(OH)<sub>2</sub>, Ni(OH)<sub>2</sub>, and Pb(OH)<sub>2</sub>; thus, it is not able to bind to the functional groups present in or on the cell wall [36]. Considering these outcomes, the biosorption of the examined metal ions on the *S. cerevisiae* biomass happens with the highest efficacy at a pH of 5, and this value was the most suitable and was utilized in all other experimental studies.

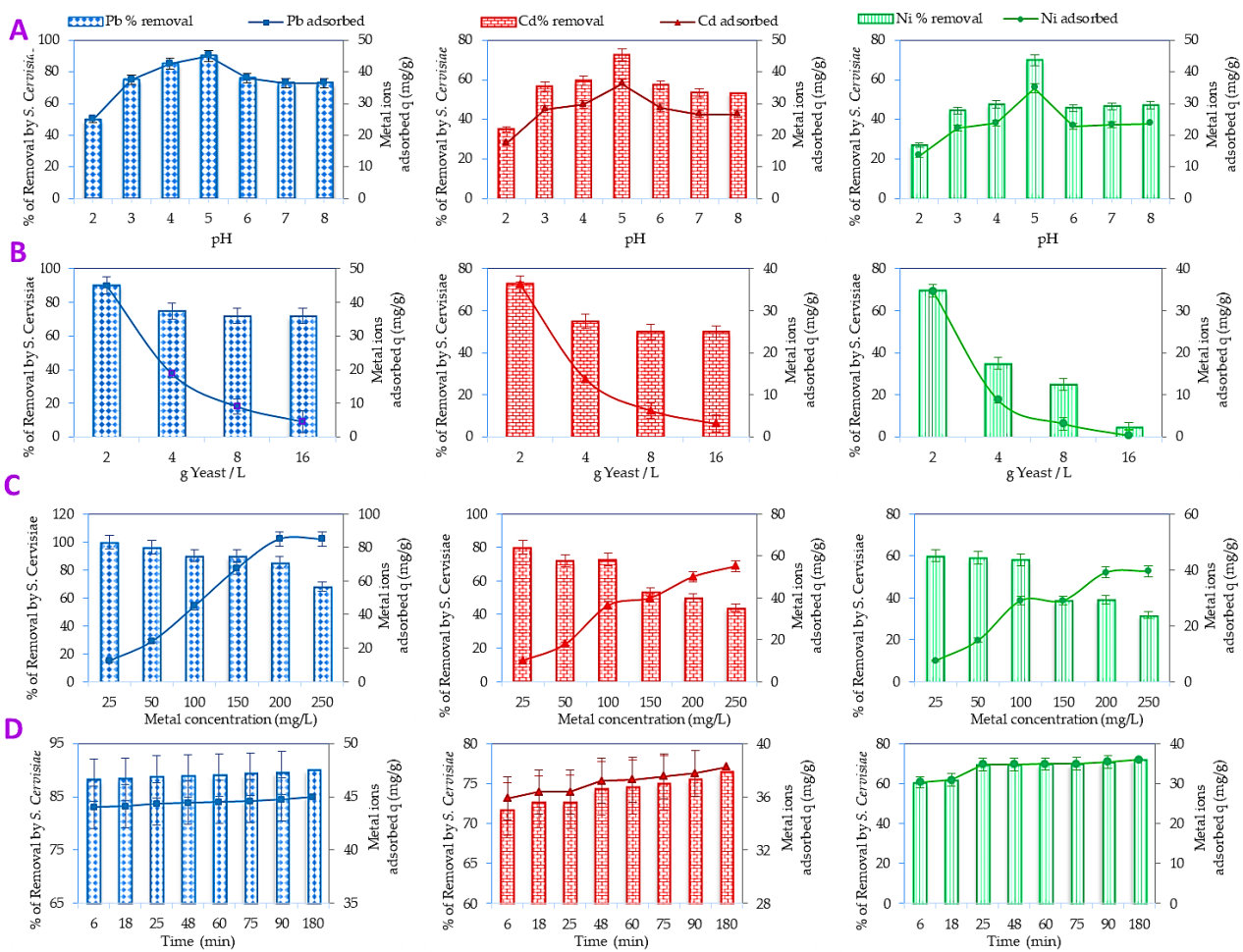


**Figure 2.** Impact of pH (A), biosorbent dose (B), initial concentration (C), and (D) time on the removal efficiency and adsorption capacity of Cd(II), Pb(II), and Ni(II) ions on *S. cerevisiae* yeast cells. For (A,B,D) the biosorbent concentration was 0.5 g/250 mL (dry mass/volume), and the initial metal concentration 100 mg/L, 25 °C, 150 rpm and 2 h. Error bars represent standard deviation.

### 3.1.2. Impact of Biosorbent Dose

The influence of various biomass (*S. cerevisiae*) doses on the biosorption performance for Cd(II), Pb(II), and Ni(II) was investigated and is delineated in Figure 2B. It can be seen from Figure 2B that the biosorption capacity is greatest at a biosorbent dosage of 2 g/L. As the biosorbent dose increased, the biosorption capacity reduced, while the efficacy of biosorption increased. The variation in biosorption processes is explained by the lessening in the ratio among the number of ions and the number of biosorbent functional groups [54]. Furthermore, raising the biosorbent dosage to 2–4 g/L results in a negligible advancement (up to 10%) in the metal ions' removal percentage. Hence, a dosage of 2 g/L was sufficient for the biosorption of the investigated metal ions on *S. cerevisiae* and was deemed optimal.

### 3.1.3. Impact of Initial Concentration and Biosorption Isotherms

Figure 2C displays the efficiency of *S. cerevisiae* as an adsorbent for each metal ion in adsorption experiments at concentrations ranging from 25 to 250 mg/L. The outcomes demonstrated that the capacity of biosorption (removal ratio) enhances, while the biosorption yield of biomass reduces as the initial metal ions' concentration increases. While the pathway of biosorption of the investigated metal ions is reliant on their initial concentration, at low concentrations, metal ions are biosorbed by specific active sites on *S. cerevisiae*, while with increasing metal ion concentrations, the specific sites are somewhat saturated. Our results were reinforced by the investigation of Martins et al. [55] in which they exhibited

that the adsorption rate significantly reduced with increasing elemental Cd(II), Pb(II), and Ni(II) concentrations up to 100 mg/L.

Linear Langmuir and Freundlich biosorption isothermal models for the trace elements investigated by *S. cerevisiae* are exhibited in Figure 3A,B, respectively. Table 2 shows the model parameters ( $K_d$ ,  $q_{max}$ ,  $K_f$ , and  $n$ ) estimated from the experimental and model isotherms for investigated metal ions. Langmuir isotherms provide the best fit for the computed values for *S. cerevisiae*; that conclusion can be based on a high  $R^2$  correlation coefficient ( $R^2 \geq 0.99$ ) compared to the  $R^2$  of another isotherm ( $R^2 = 0.96$ – $0.98$ ). During the adsorption process, the investigated ions cover the adsorbent with monolayer sorption onto a surface with a finite number of matching sorption sites.

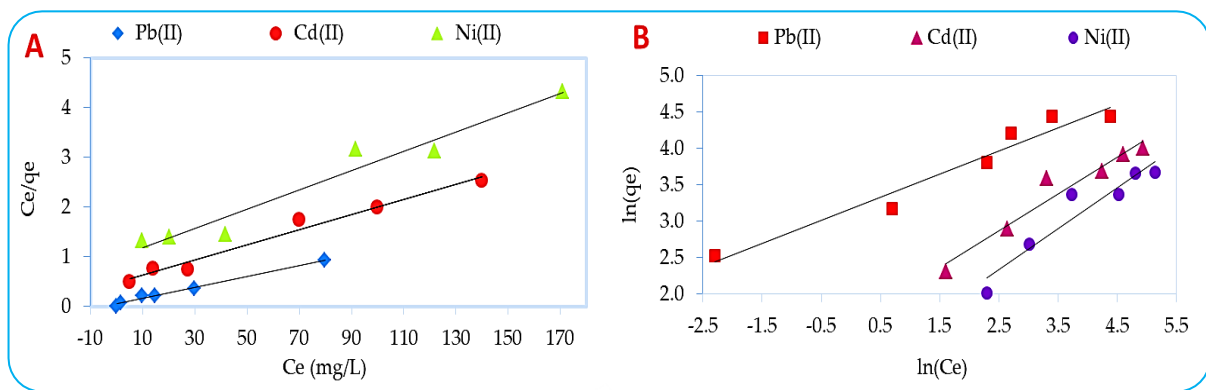


**Figure 3.** (A) Langmuir and (B) Freundlich biosorption isotherms of Cd(II), Pb(II), and Ni(II) by *S. cerevisiae*.

**Table 2.** Isotherm Model Parameters for Adsorption of Cd(II), Pb(II), and Ni(II) on *S. cerevisiae* using Langmuir and Freundlich Isotherms.

Parameters	Langmuir Model			Freundlich Model			
	$q_{max}$ (mg/g)	$b = (1/K_d)$	$R^2$	RL	$K_f$ (L/g)	$n$	$R^2$
Cd(II)	65.36	0.032	0.98	0.11–0.56	4.95	1.98	0.94
Pb(II)	90.09	0.193	0.99	0.02–0.17	23.69	3.14	0.94
Ni(II)	51.55	0.020	0.95	0.17–0.67	2.50	1.77	0.90

The highest biosorption capacity ( $q_{max}$ ) for Cd(II), Pb(II), and Ni(II) ions is 65, 90, and 51 mg/g, respectively. The fundamental isothermal characteristics of Langmuir’s are evident in expressions of RL (a dimensionless constant separation factor), known as  $RL = \frac{1}{(1+bC_0)}$  in the range  $0 < RL < 1$ , reflecting the appropriate adsorption process [56]. As indicated by the low RL values for lead (0.02–0.17) and the high RL values for nickel (0.67–0.17), the yeast cells showed a high and low affinity for  $Pb^{2+}$  and  $Ni^{2+}$ , respectively. However, the values of RL for any tested metal ion were found in the range  $0 < RL < 1$ , confirming that the adsorption process was suitable for the examined metal ions. In addition, the value of  $1/n < 1$  calculated from the Freundlich isotherm model confirms that the process is chemical [57].

Table 3 presents a comparison of the  $q_{max}$  obtained from the Langmuir isotherm model in the literature data [33,42,47,58–62] with this investigation for various adsorbents to Cd(II), Pb(II), and Ni(II). The  $q_{max}$  value for Cd(II) was found to be 65.36, which was higher than that of *B. thuringiensis*-remediated wastewater [58], ethanol-treated yeast [47], and EDTA-treated yeast [60]. The  $q_{max}$  value was found to be 90.09 mg/g for Pb(II), which was higher than that of *P. chrysosporium*-treated wastewater [59], a bioreactor biosorption system [42], and ethanol-treated *S. cerevisiae* [47], but less than that of EDTA-treated yeast [60]. The  $q_{max}$  was estimated to be 51.55 mg/g for Ni(II), which was near the value estimated by Guler

and Ersan [61], and was higher the value Özer and Özer [33] and Guler and Sarioglu [62]. The  $q_{\max}$  for the prepared yeast was higher and lower, respectively, than the  $q_{\max}$  found in the literature, probably attributed to the condition of the reaction, the treatment materials, the source of yeast, the media used to culture the yeast, and the inactivation. All of the above confirmed that culturing yeast on YPD and drying it at 25 °C enhanced its properties more than the studies in the literature for the biosorption of Cd(II) Pb(II), and Ni(II) ions.

**Table 3.** The maximum adsorption capacity ( $q_{\max}$ ) of various biosorption capacities of biomass discovered in this research was compared to those published in the literature for Cd(II), Pb(II), and Ni(II), respectively.

Metal Ions	Biomass	$q_{\max}$ (mg/g)	Reference
Cd(II)	<i>B. thuringiensis</i>	59.17	[58]
	<i>S. cerevisiae</i>	31.75	[47]
	<i>P. chrysosporium</i>	27.79	[59]
	<i>S. cerevisiae</i>	32.26	[60]
	<i>S. cerevisiae</i>	65.36	This study
Pb(II)	<i>S. cerevisiae</i>	72.46	[42]
	<i>B. thuringiensis</i>	30.76	[58]
	<i>P. chrysosporium</i>	85.57	[59]
	<i>S. cerevisiae</i>	60.24	[47]
	EDTA-treated <i>S. cerevisiae</i>	200	[60]
	<i>S. cerevisiae</i>	90.09	This study
Ni(II)	<i>S. cerevisiae</i> nZVI	54.23	[61]
	<i>S. cerevisiae</i>	21.39	[62]
	<i>S. cerevisiae</i>	46.30	[33]
	<i>S. cerevisiae</i>	51.55	This study

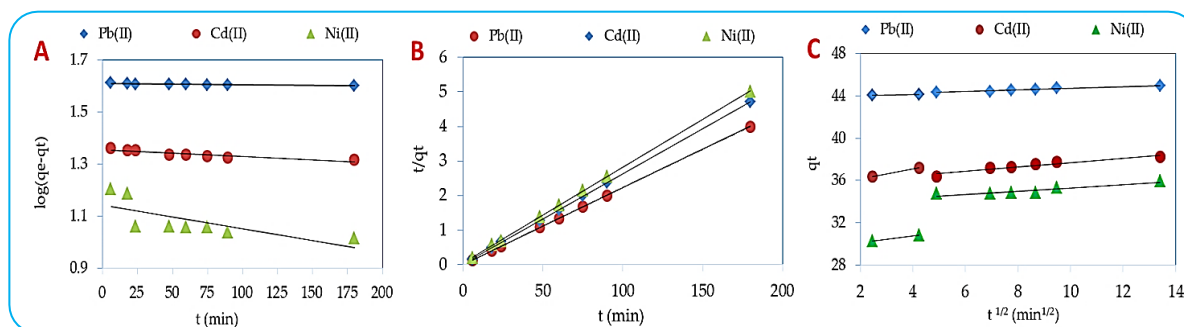
### 3.1.4. Impact of Time on Biosorption and Kinetic Isotherms

The consequence of the biosorption kinetics of Cd(II), Pb(II), and Cu(II) ions at various intervals time for *S. cerevisiae* is shown in Figure 2D. In the range of 6 min and 18 min, the ions are rapidly biosorbed by the *S. cerevisiae*, and the state of equilibrium arrives at 25 min for the examined metal ion. Those returning to the functional groups of *S. cerevisiae* are uncovered, and the metal ions are rapidly bound, regardless of their nature. After 48 min, there was no further increase in biomass biosorption capacity for ions, and the removal percentage did not change significantly until 180 min. This implies that the entire surface of the *S. cerevisiae* was coated. Hence, metal ions struggle to identify active centers accessible for binding, resulting in a slow increase in biosorption capacity. Thusly, a contact time of 25 min is adequate to attain equilibrium in the case of the biosorption of the three examined metal ions on *S. cerevisiae*.

The regression coefficient ( $R^2$ ) values clarified that the pseudo-second order (2nd) model, ( $R^2 > 0.99$ –1.00) was the best-fitting model compared with pseudo-first-order rate kinetics ( $R^2 > 0.54$ –88), and the intraparticle diffusion model ( $R^2 > 0.85$ –0.96), see Table 4 and Figure 4A–C. The rate constant of the pseudo-second-order was in the range of 0.013–0.049 g/mg/min, see Table 4. These outcomes were supported by Amirnia et al. [42]. Thus, in this case, the limiting rate of the biosorption reaction may be chemisorption since the removal of the investigated metal ions occurs most often via surface complexation reactions at specific biosorption sites [63]. Thusly, the metal ions' retention on the surface of *S. cerevisiae* is accomplished via chemical interactions that include two active centers in good geometric positions. The proclivity of metal ions to cooperate with the binding sites of *S. cerevisiae*, depicted by  $k_2$ , indicates that Pb(II) ions are most effectively retained (0.049 g/mg min), accompanied by Cd(II) ions (0.021 g/mg min), and finally Ni(II) ions (0.013 g/mg min).

**Table 4.** Kinetic parameters of the Cd(II), Pb(II), and Ni(II) removal by *S. cerevisiae* biomass.

Ions	Pseudo-First-Order			Pseudo-Second-Order				Intraparticle					
	$q_e$ (mg/g)	$K_1$ (min <sup>-1</sup> )	$R^2$	$v_2$ (mg/gmin)	$q_e$ (mg/g)	$k_2$ (g/mg min)	$R^2$	Zone I			Zone II		
								$K_d$ (mg/g/min <sup>0.5</sup> )	I	$R^2$	$K_d$ (mg/g/min <sup>0.5</sup> )	I	$R^2$
Pb(II)	40.9	0.0001	0.88	99.0	45.05	0.049	1.00	0.05	43.93	0.99	0.08	43.16	0.96
Cd(II)	22.8	0.0007	0.84	30.7	38.5	0.021	0.99	0.26	35.24	0.99	0.21	35.61	0.91
Ni(II)	13.9	0.0021	0.54	17.5	36.2	0.013	0.99	0.32	29.49	0.96	0.15	33.80	0.85

**Figure 4.** Plot of pseudo-first order equation (A), pseudo-second order equation (B), and intraparticle (C) of Cd(II), Pb(II), and Ni(II) ions' adsorption by *S. cerevisiae* biomass.

### 3.1.5. Impact of Temperature on Biosorption and Thermodynamic Studies

The thermodynamic parameters Gibbs free energy ( $\Delta G^\circ$ ), enthalpy ( $\Delta H^\circ$ ), and entropy ( $\Delta S^\circ$ ) clarify how spontaneous the biosorption process is, see Table 5. The equilibrium constant ( $K$ ) was estimated using the equation:  $\Delta G = -RT \ln K$  at different temperatures (15–40 °C). The greatest biosorption capacity for the examined ions by *S. cerevisiae* was achieved at a temperature of 25 °C; after that, the %RE and the biosorption capacity were constant, see Figure 5A. The negative values of  $\Delta G$  for the tested metal ions proved that the biosorption process was spontaneous. The  $\Delta H^\circ$  and  $\Delta S^\circ$  for the biosorbent were calculated utilizing the Van't Hoff plot of  $\ln K$  against  $1/T$ , see Figure 5B. The positive values of the  $\Delta S^\circ$  for all trials of metal ions demonstrated an expansion in irregularity at the solid/liquid interface during the biosorption process. The negative values of  $\Delta G^\circ$ , while  $\Delta S^\circ$  had positive values, were supported by Gialamoudis et al. [64]. The positive  $\Delta H^\circ$  for the trial metals revealed that the biosorption process was endothermic.

**Table 5.** Values estimated from the thermodynamic analysis.

Temperature T (K)	288	293	298	303	313
Pb(II)					
Gibbs free energy $\Delta G^\circ$ (kJ mol <sup>-1</sup> )	-2.62	-2.99	-3.36	-3.73	-4.47
Entropy $\Delta S^\circ$ (kJ mol <sup>-1</sup> K <sup>-1</sup> )			0.073		
Enthalpy $\Delta H^\circ$ (kJ mol <sup>-1</sup> )			18.64		
Cd(II)					
Gibbs free energy $\Delta G^\circ$ (kJ mol <sup>-1</sup> )	-0.66	-0.96	-1.25	-1.55	-2.14
Entropy $\Delta S^\circ$ (kJ mol <sup>-1</sup> K <sup>-1</sup> )			0.059		
Enthalpy $\Delta H^\circ$ (kJ mol <sup>-1</sup> )			16.39		
Ni(II)					
Gibbs free energy $\Delta G^\circ$ (kJ mol <sup>-1</sup> )	-0.05	-0.33	-0.61	-0.89	-1.45
Entropy $\Delta S^\circ$ (kJ mol <sup>-1</sup> K <sup>-1</sup> )			0.056		
Enthalpy $\Delta H^\circ$ (kJ mol <sup>-1</sup> )			16.16		

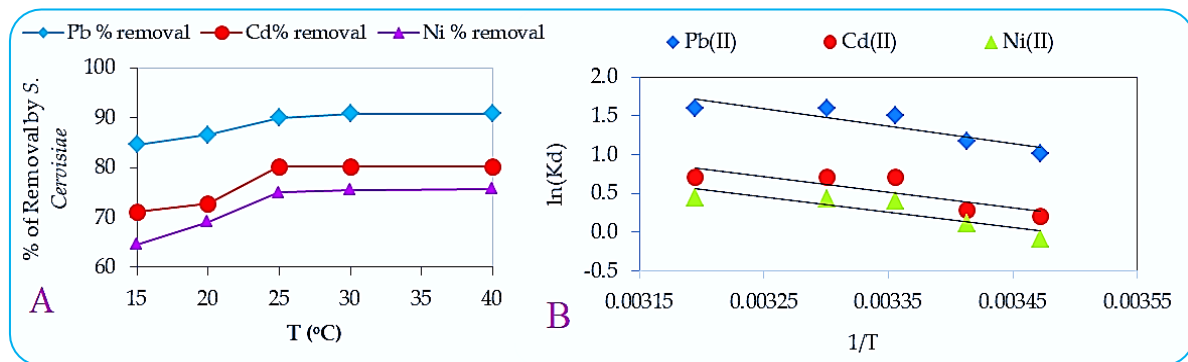


**Figure 5.** (A) Removal efficiency versus temperature, and (B)  $\ln(K_d)$  versus  $1/T$  of Cd(II), Pb(II), and Ni(II) ions' adsorption by *S. cerevisiae* biomass.

### 3.2. Mechanism of *S. cerevisiae*

#### 3.2.1. XRD of *S. cerevisiae*

Figure 6A,D elucidates the chemical nature of yeast cells bound to native lead, cadmium, and nickel, respectively. Figure 6A for native *S. cerevisiae* biomass is expected to be amorphous. Figure 6B depicts lead accumulation in five distinct peaks at  $2\theta$ ;  $21.67^\circ$ ,  $27.71^\circ$ ,  $31.31^\circ$ ,  $41.19^\circ$ , and  $44.08^\circ$ , corresponding to respective d-spacing 4.15, 3.40, 3.36, and 2.19 Å. Based on spacing values, these peaks are ascribed to the presence of crystalline lead sulfate compounds ( $\text{Pb}_3\text{O}_2\text{SO}_4$  and  $\text{Pb}_2\text{OSO}_4$ ,  $\text{Pb}(\text{SO}_4)$  and  $\text{Pb}_2\text{O}_4$ ). Extracellular Pb-containing minerals are lead sulfate [48].

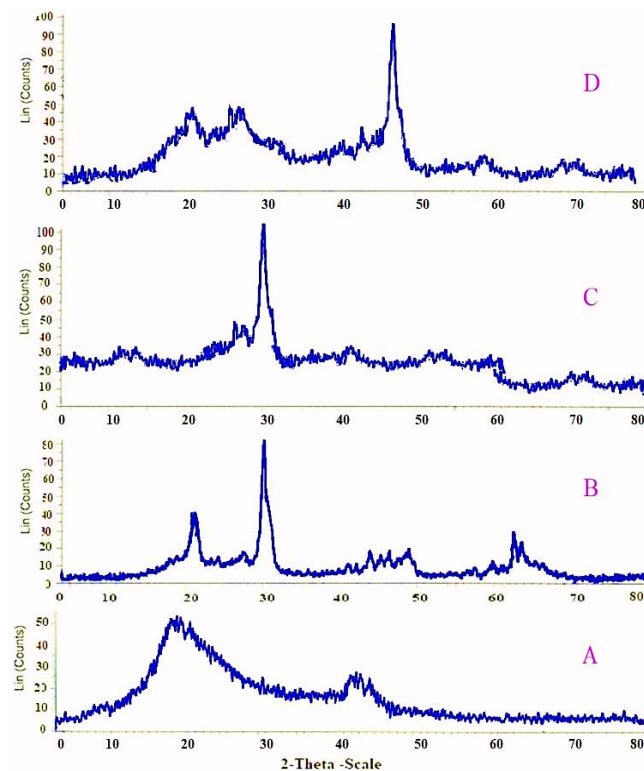


**Figure 6.** XRD analysis of (A) native, (B) lead-loaded, (C) cadmium-loaded, (D) nickel-loaded *S. cerevisiae* biomass.

Figure 6C presents the XRD pattern of *S. cerevisiae* loaded by cadmium, which shows distinct peaks at  $2\theta$ ,  $43^\circ$ , and  $52.28^\circ$ , which belong to (110) and (111) planes of the  $\text{Cd}(\text{OH})_2$  crystalline structure with a hexagonal phase, which concurs with JCPDS card No. 31-0228, while the distinct peak at  $30.33^\circ$  belongs to the  $\text{Cd}(\text{OH})_2$  monoclinic phase, which is ori-

ented along (110) reflection planes as per JCPDS card No. 84-1767. The low reflection at  $2\theta$   $27.4^\circ$ , corresponding to the plane (210), is attributed to the presence of cadmium chloride phosphate (JCPDS cards 29-0254 and 30-0206). Extracellular Cd-containing minerals (cadmium hydroxide and cadmium chloride phosphate) were observed on the cell wall.

In Figure 6D, the mean peak at  $47.8^\circ$  is indexed to the (132) and corresponds to  $1.90 \text{ \AA}$ , and the other peak at  $22.18^\circ$  is indexed to the (130) corresponding to the respective d-spacing  $4.005 \text{ \AA}$ , which indicate the presence of nickel orthophosphate octahydrate ( $\text{Ni}_3(\text{PO}_4)_2 \cdot 8\text{H}_2\text{O}$ ) (JCPDS No.19033-89-7) and hexagonal phase  $\text{Ni}_2\text{P}$  (JCPDS No. 74-1385,  $P62m$ ,  $a = 5.859 \text{ \AA}$ ,  $c = 3.382 \text{ \AA}$ ), while the diffraction peaks at  $43.85^\circ$ ,  $42.6^\circ$ , and  $59^\circ$  are indexed to the (100), (111), and (102), which belong to  $\text{Ni}_2\text{O}_3$  (JCPDS 14-0481),  $\text{NiO}_2$  (JCPDS 89-8397), and Ni (JCPDS 89-7129), respectively. The extracellular Ni-containing minerals are nickel phosphide, nickel orthophosphate octahydrate, nickel oxide, and nickel dioxide.

### 3.2.2. FTIR of *S. cerevisiae* and Its Impact on Biosorption of Investigated Metal Ions

To investigate the impacts of Cd(II), Pb(II), and Ni(II) on the properties of cell walls, the *S. cerevisiae* functional groups were investigated with and without the examined metal ions using FTIR analysis. The infrared spectra FTIR of native *S. cerevisiae* and metal-loaded ones were recorded over the range of  $300\text{--}4000 \text{ cm}^{-1}$ . Native *S. cerevisiae* biomass displays a different FTIR spectrum in Figure 7A; the mean peak at  $3413 \text{ cm}^{-1}$  is characteristic of hydroxyl O-H and N-H stretching vibrations, while the peak at  $2928 \text{ cm}^{-1}$  refers to the methyl groups' (C-H) asymmetric stretching [48]. Furthermore, the band at  $1644 \text{ cm}^{-1}$  proved the vibration C=O of the acetyl group and the deformation N-H of the amide (II) group at  $1550 \text{ cm}^{-1}$  refers to the stretching (C-N, and N-H) of amides II from proteins, and  $1380 \text{ cm}^{-1}$  belonged to the carboxyl group appearance ( $\text{COO}^-$ ) in proteins. In addition, the band that appeared at  $1239 \text{ cm}^{-1}$  refers to a strong symmetrical stretching vibration of the phosphodiester group [ $\text{vs}(\text{-PO}_2^{2-})$ ] in DNA and RNA and phospholipids groups, and  $1072 \text{ cm}^{-1}$  appertains to the  $\beta(1\rightarrow3)$  stretching of glucan and S=O. Finally, the peak at  $537 \text{ cm}^{-1}$  was assigned to an asymmetrical stretching vibration of  $\text{PO}_4^{3-}$ , which reveals that the phospholipid bi-layers also exist in yeast cells. From the abovementioned, the primary functional groups of the native fungal cells of *S. cerevisiae* are the hydroxyl, amide, acetyl, methyl/methylene, carboxyl, phosphoryl, and nitro groups. All of these functional groups or active binding sites can be utilized to assess the efficacy of the biosorption process since they are engaged in the retention of metal ions from the solution [48].

On the other hand, the changes in the vibrational frequencies identified through FTIR clarified the engagement of the *S. cerevisiae* cell wall in Pb(II) removal (Figure 7B). The biosorption of Pb(II) on the *S. cerevisiae* surface led to a shift in wavelength by  $-10$  to  $-1 \text{ cm}^{-1}$ . When compared to the original sample, the peak  $1239 \text{ cm}^{-1}$  had not changed, indicating that the lead atoms did not bind to the phosphate group. However, some peaks had a slight shift to a lower wavelength ( $3413\text{--}3407$ ,  $2928\text{--}2926$ ,  $1644\text{--}1641$ ,  $1550\text{--}1543$ ,  $1380\text{--}1373$ ,  $1072\text{--}1062$ , and  $537\text{--}535 \text{ cm}^{-1}$ ), suggesting the intervention of hydroxyl, methyl, acetyl, carboxyl, sulfide, Pb-O, and ring deformation groups during Pb(II) adsorption [48,65].

Furthermore, the FTIR spectral analysis of *S. cerevisiae* biomass cadmium-loaded in Figure 7C displays a shift in the wavelength from  $-19$  to  $+11 \text{ cm}^{-1}$ . When compared to the native cells, the peaks displayed at  $1072$  and  $1550 \text{ cm}^{-1}$  disappeared completely after Cd(II) ions, which means that amides II and S=O participated in the biosorption of cadmium ions. Some peaks had a slight shift to a lower wavelength ( $1380\text{--}1378$ ,  $1644\text{--}1625$ , and  $537\text{--}520 \text{ cm}^{-1}$ ), whereas others had a significant shift to a higher wavelength in peaks ( $3413\text{--}3420$ ,  $2928\text{--}2930$ , and  $1239\text{--}1250 \text{ cm}^{-1}$ ) after Cd(II) treatment. The shift to low and higher wavelengths could imply that the carboxyl, acetyl, methyl, hydroxyl, and phosphate groups were engaged with the binding of Cd(II) on the cell wall [66].

The FTIR spectral analysis of *S. cerevisiae* biomass nickel-loaded in Figure 7D displays a shift in wavelength by  $-23$  to  $+2 \text{ cm}^{-1}$ . The peaks displayed at  $2350$  and  $535 \text{ cm}^{-1}$  vanished completely when compared to the native sample, implying that the phosphate group participated in nickel biosorption. The peak  $1072 \text{ cm}^{-1}$  demonstrated no difference

with respect to original yeast because nickel atoms did not bind to the sulfide and glucan groups. Furthermore, significant shifts to a low wavelength in peaks  $3413\text{--}3395\text{ cm}^{-1}$ ,  $2928\text{--}2924$ ,  $1644\text{--}1621$ ,  $1550\text{--}1541\text{ cm}^{-1}$ , and  $1380\text{--}1373\text{ cm}^{-1}$  after Ni(II) treatment might imply the involvement of the methyl, hydroxyl, acetyl, amide, and carboxyl groups, while a shift to a higher wavelength in peak  $1239$  to  $1241\text{ cm}^{-1}$  suggests the phosphate group was involved in the binding of Ni(II) on the cell wall [67].

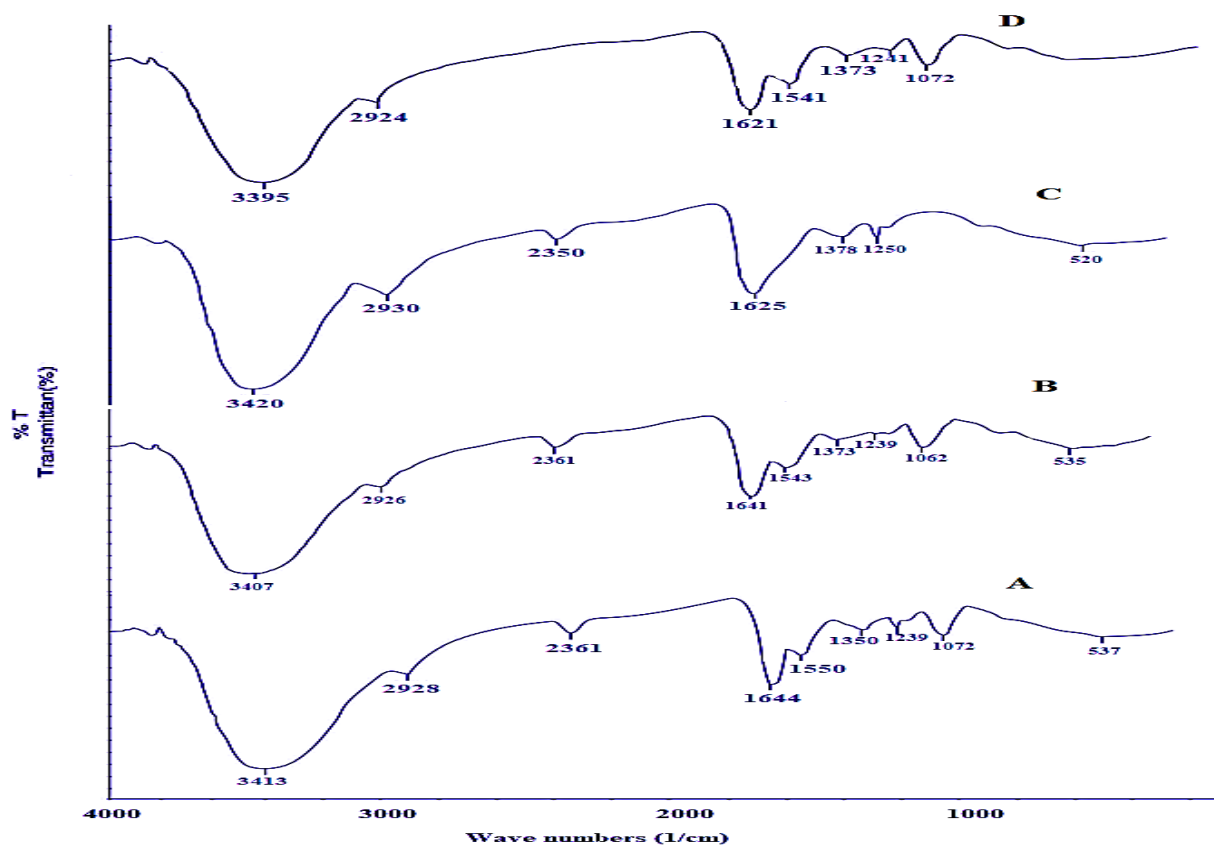


**Figure 7.** FTIR spectrum of raw *S. cerevisiae* (A) and lead- (B), cadmium- (C), and nickel (D)-loaded *S. cerevisiae*.

Finally, there was a shift to low and high wavelengths in the peak bands of treated *S. cerevisiae* stacked with the investigated metal ions. These deformations of peaks presented in the FTIR spectrum can be surveyed as evidence of biosorption. In addition, no new absorption bands were found to be pertinent for showing that the biosorption of investigated metal ions is not involved in the formation of covalent bonds and that it is performed predominantly through ion-exchange interactions (that are electrostatic) [48,65–67].

### 3.2.3. Surface Area of *S. cerevisiae*

The previously mentioned features of yeast by FTIR with its large surface area ( $252.6\text{ m}^2/\text{g}$ ) make it capable of holding heavy metals through biosorption, see Table 6. The nitrogen adsorption–desorption isotherms of the raw *S. cerevisiae* and Pb-loaded *S. cerevisiae* are identified as type IV following the IUPAC “International Union of Pure and Applied Chemistry” classification (Figure 8A,B). This kind of isotherm is characteristic of mesoporous adsorbents for the *S. cerevisiae* and Pb-loaded *S. cerevisiae* and is preferred for the process of ion exchange as it provides more access sites for sorbate cations to reach the internal porosity. The surface area of yeast was reduced from  $252.6\text{ m}^2/\text{g}$  to  $225\text{ m}^2/\text{g}$  after the biosorption of Pb(II) (Table 6). The depletion in surface area can be credited to the creation of new surfaces in inactivated *S. cerevisiae* by physical entrapment and ion exchange.

The prepared yeast has a higher surface area than is found in the literature [24,54], which confirms the higher result of  $q_{\max}$  than is found in the literature.

**Table 6.** Brunauer–Emmett–Teller (BET) analysis for raw and Pb(II)-*S. cerevisiae* biomass.

	Surface Area	Average Particle Size	Total Pore Volume
<i>S. cerevisiae</i>	252.6 m <sup>2</sup> /g	4.60667 nm	0.581792 cc/g (cm <sup>3</sup> /g)
Pb(II)-loaded <i>S. cerevisiae</i>	221.97 m <sup>2</sup> /g	4.60667 nm	0.511272 cc/g (cm <sup>3</sup> /g)

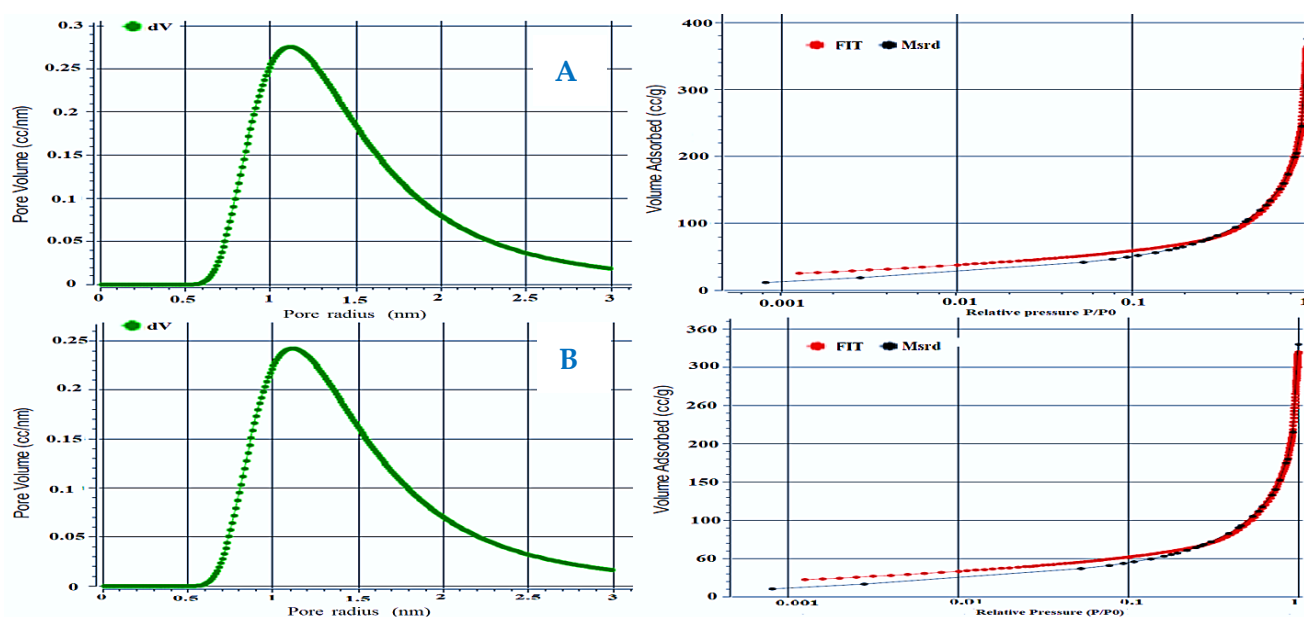


**Figure 8.** N<sub>2</sub> sorption isotherms for the hydrothermal alkali-activation products of *S. cerevisiae* (A) and Pb-loaded *S. cerevisiae* biomass (B).

### 3.2.4. TEM of *S. cerevisiae*

Transmission electron microscopy (TEM) was utilized to pinpoint mineral phases inside and on cell walls as well as their morphology. TEM was performed to observe the extent of morphology differences before and after the biosorption of metal by *S. cerevisiae* (Figure 9A,B). It was evident that the *S. cerevisiae* morphology can facilitate the sorption of Pb<sup>2+</sup> because of its cellular surface being smooth with no membrane dentitions and the uniform electron-dense area across the monocyte body of the stain. After the biosorption of Pb(II), it was deposited inside and outside the *S. cerevisiae* and formed an irregular surface of the biosorbent materials that had fractions of mesoporous particles (Figure 9B). Various examinations have affirmed that numerous fungi can accumulate significant trace elements in their cells, without annihilating the integrity of the cells [68–70]. Intracellular Pb(II) transport occurs through binding to intracellular metal or sequestering sites that have a stronger affinity than cell surface binding sites, and this provides a driving force for intracellular biosorption [68–70]. Accordingly, the fungi developed a mechanism to remove toxins within the cell. Hence, the efficiency of *S. cerevisiae* required a sufficient morphology for the biosorption of mineral particles formed within cells to create a crystalline structure.

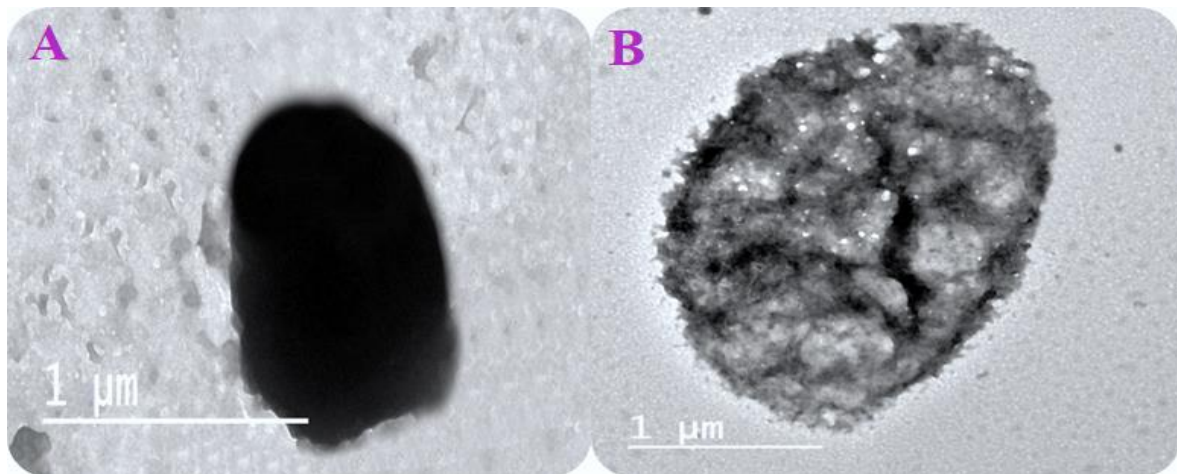


**Figure 9.** TEM images where (A) TEM native *S. cerevisiae* and (B) loading with lead.

### 3.3. Biomass Regeneration (Desorption)

Metal desorption from the immobilized yeast cells can result in biomass regeneration as well as valuable metal reclamation. Desorption is necessary when the preparation and production of biosorbent is expensive.

In the present investigation, various types of desorbents solutions ( $H_2O$ ,  $NH_4NO_3$ , EDTA, and citric acid) were used in three cycles to desorb Cd(II), Pb(II), and Ni(II) ions from immobilized *S. cerevisiae*, see Figure 10. The obtained data show the degree of desorption of Cd(II), Pb(II), and Ni(II) from immobilized *S. cerevisiae*. EDTA and citric acid characterize the highest desorption ( $80 \pm 4$ ,  $90 \pm 5\%$ , respectively) because of their ability to form a wide variety of complexes as chelating agents. The EDTA can desorb not only the metal associated with physical entrapment, exchanged but also metal complexes with functional groups, while citric acid has the ability to desorb metal associated with physical entrapment, exchanged, complexes, and parts from the residual metals, which are bio-accumulated. It is suggested that  $H_2O$  (12–20%) and  $NH_4NO_3$  (38–45%) display the lowest and medium, respectively, desorption capacities to Pb(II), Cd(II), and Ni(II) ions from *S. cerevisiae*. The lowest desorption by  $H_2O$  can be credited to the physical entrapment in which the metal ions are easily susceptible to desorption by water because they weakly bind metals to the cell surface, while the medium desorption using  $NH_4NO_3$  can be ascribed to the ion exchange with  $Na^+$ ,  $Ca^{2+}$ ,  $K^+$ , and  $Mg^{2+}$  on the cell *S. cerevisiae* wall.

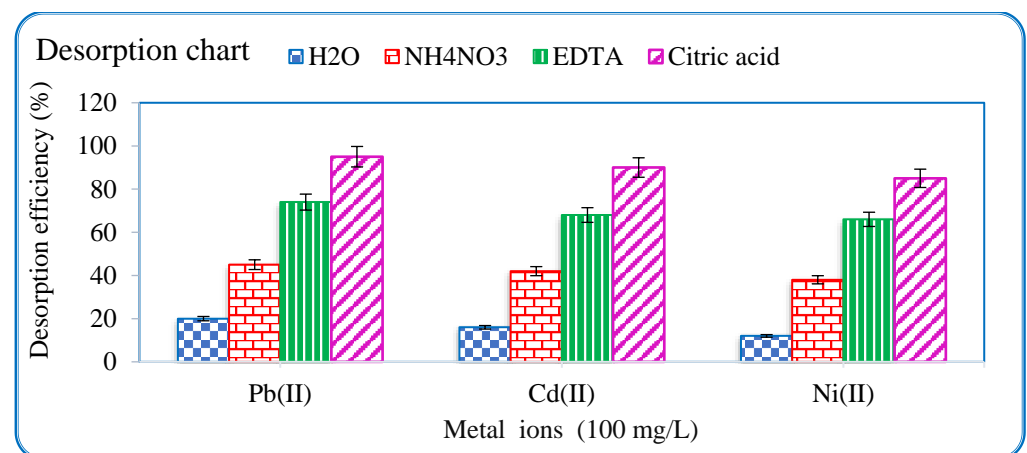


**Figure 10.** Desorption efficiency (%) of metal ions (100 mg/L for each) biosorbed by immobilized *S. cerevisiae* yeast cells by  $H_2O$ ,  $NH_4NO_3$ , EDTA, and citric acid. Error bars represent standard deviation.

### 3.4. Corn Industrial Effluent Treatment

The outcomes of the physicochemical analyses of wastewater samples from the corn factory are displayed in Table 7. The normality test was applied to the researched variables and exhibited that the test showed significant values ( $p > 0.05$ ) for all variables, which affirmed that the examined water quality variables have a normal distribution. The comparison of the two approaches: raw *S. cerevisiae* AP1 and immobilized *S. cerevisiae* AP2 (fixed-bed column) for the treatment of effluent wastewater are displayed in Table 7. Statistically, the analytical data indicated that both the *S. cerevisiae* and fixed-bed column utilized for wastewater remediation demonstrated significant differences ( $<0.05$ ) for all examined water quality variables. The pH of the solution was slightly alkaline, ranging between 7.6 and 8.2. *S. cerevisiae* showed good activity for the removal of calcium, sodium, potassium, and magnesium ions, with significant variation ( $p < 0.05$ ) from food effluent.

**Table 7.** Water quality parameters of raw wastewater, and treated water after the application of *S. cerevisiae*,  $p$ -value, and their removal efficiency (RE%). (n = 3 samples).

Parameters *	Raw Wastewater				Treated Water with <i>S. cerevisiae</i> (AP1)				Treated Water with <i>S. cerevisiae</i> Uploaded on Calcium Alginate (AP2)					
	Min	Max	Average	$p$	Min	Max	Average	$p$	RE (%)	Min	Max	Average	$p$	RE (%)
pH	6.7	6.9	6.8 ± 0.11 <sup>B</sup>	Less than 0.05	7.5	7.7	7.6 ± 0.10 <sup>A</sup>	Less than 0.05	−11.8	8.1	8.2	8.2 ± 0.01 <sup>A</sup>	Less than 0.05	−11.6
Ca <sup>2+</sup>	400.5	483.8	453.3 ± 45 <sup>A</sup>		11.6	13.9	13.1 ± 1.27 <sup>B</sup>		97.1	12.6	25.5	20.5 ± 6.9 <sup>B</sup>		95.5
Mg <sup>2+</sup>	1148.6	1332.8	1255.0 ± 49 <sup>A</sup>		112.5	131.3	120.5 ± 9.73 <sup>B</sup>		90.4	118.9	152.3	139.3 ± 17.9 <sup>B</sup>		88.9
Na <sup>+</sup>	1740.0	1918.5	1803.6 ± 99 <sup>A</sup>		54.3	59.6	56.1 ± 3.06 <sup>B</sup>		96.9	54.3	105.8	85.8 ± 27.6 <sup>B</sup>		95.2
K <sup>+</sup>	763.9	1527.8	1085.5 ± 395 <sup>A</sup>		17.5	35.1	25.0 ± 9.11 <sup>B</sup>		97.7	22.0	50.9	39.7 ± 15.5 <sup>B</sup>		96.3
BOD	8800.0	9220.0	9006 ± 210 <sup>A</sup>		179.9	360.3	240.1 ± 104 <sup>B</sup>		98.0	105.3	244.9	190.7 ± 355 <sup>B</sup>		93.8
COD	11,200	12,100	11,766 ± 493 <sup>A</sup>		400.0	435.8	423.9 ± 20 <sup>B</sup>		96.6	171.3	772.0	558.0 ± 324 <sup>B</sup>		93.5
Cd <sup>2+</sup>	13.50	16.70	15 ± 1.5 <sup>A</sup>		0.151	0.184	0.167 ± 0.02 <sup>B</sup>		98.9	0.152	0.591	0.420 ± 0.24 <sup>B</sup>		97.2
Pb <sup>2+</sup>	2.87	3.33	3.04 ± 0.2 <sup>A</sup>		0.029	0.035	0.031 ± 0.002 <sup>B</sup>		99.0	0.2	0.6	0.4 ± 0.05 <sup>B</sup>		97.3
Ni <sup>2+</sup>	12.00	24.00	18.3 ± 6 <sup>A</sup>		0.253	0.509	0.387 ± 0.1 <sup>B</sup>		97.9	<DL	0.1	0.1 ± 0.280 <sup>B</sup>		96.2

\*: The units of variables in Table 7 are mg/L, pH is unitless dimension. Negative values are an indication of the increased pH after the application of treatment. Data represented as mean ± SD of 3 samples. The single alphabetical letters (<sup>A</sup> and <sup>B</sup>) in the same column for each studied parameter are significantly different ( $p < 0.05$ ).

On the other hand, it was proved that the competitive outcomes of the biosorption of metals by *S. cerevisiae* followed the order: Pb(II) > Cd(II) > Ni(II). Because lead has a smaller ionic cation radius (4.01 for lead [18]), it has a higher probability of being biosorbed by *S. cerevisiae* than the other metal ions. For a single metal at 25 mg/L, simulated solutions of the efficacy of the removal of Ni(II) and Cd(II) were viewed at 60 and 80%, respectively, and almost 99% for Pb(II), as discussed previously in that investigation, while in food effluent, the efficacy of elimination by *S. cerevisiae* was almost 100% for Pb(II), Cd(II), and Ni(II). The enhanced RE% is attributable to the concentration of a single metal ion solution being 25 mg/L and the concentration of metal ions in real industrial effluent being extremely lower; therefore, a better RE% was taken. Biodegradation of organic compounds by *S. cerevisiae* can be seen as a better activity for the decrease in COD and BOD in the water samples, because *S. cerevisiae* has been portrayed as a strong bio-degrader, particularly for wastes rich in protein and carbohydrates [71,72].

Thusly, *S. cerevisiae* shows a superior reduction in cation, COD, BOD, Cd(II), Pb(II), Ni(II), and Zn(II).

### 3.5. Storage of the Immobilized *S. cerevisiae*

One of the prime aims of biosorption is to expand the time of storage of *S. cerevisiae*. Consequently, storage stability and reusability of the raw and immobilized system are vital for fruitful bio-treatment and for industrial remediation. As displayed in Figure 11, the immobilized *S. cerevisiae* was very steady when kept at 4 °C for 8 m (months) and showed the strength of the immobilized *S. cerevisiae* in repeated use for eight cycles, with retained RE% up to 90% for the investigated metal ions. Despite this, the raw *S. cerevisiae* was active for 2 m; after that, the RE% decreased by about 44–60%, 52–63%, and 35–48% for Pb(II), Cd(II), and Ni(II), respectively, after storage for 3–8 months. This reinforced that

the stability of immobilized *S. cerevisiae* can be attributed to the autolysis prevention by immobilization, so the immobilized yeast had a greater reduction in metal ion pollutants.

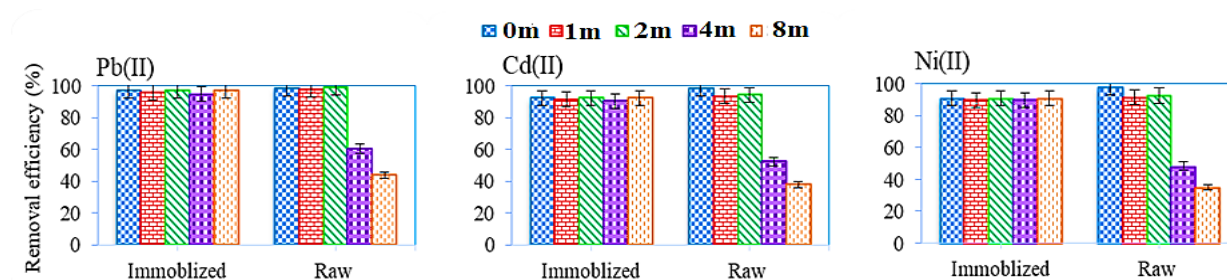


**Figure 11.** Removal efficiency (%) of Cd(II), Pb(II), and Ni(II) ions by different storage times for immobilized and raw *S. cerevisiae* yeast.

#### 4. Conclusions

The current article showed that *S. cerevisiae* was successfully grown on YPD and had the ability to reduce metal ions from water and effluent. This aspect was confirmed by XRD, TEM, BET, and FTIR outcomes. The yeast has an area of 252.6 m<sup>2</sup>/g with a mesoporous pore volume, which is higher than what is found in the literature, so the maximum biosorption capacity is 65 for Cd(II), 51 Ni(II), and 90 for Pb(II) mg/g, indicating that the grown and dried method for the yeast enhanced its character. The optimal pH for the removal of Cd(II), Pb(II), and Ni(II) from an aqueous solution is 5 at a contact time of 25 min, 2 g *S. cerevisiae*/L at 25 °C, which allowed the removal of 80, 99, and 70% (25 mg/L), and 72, 90, and 69% (100 mg/L), respectively. The Langmuir isotherm model and the second-order kinetic model were the best models for describing the spontaneous biosorption reactions of the investigated metal ions. A comparison was made between *S. cerevisiae* and a fixed-based column (packed with immobilized *S. cerevisiae*) on a real effluent. The outcomes indicated that both approaches not only remove the examined metal ions, but also cations, BOD, and COD with higher efficiency. EDTA and citric acid have proved excellent outcomes for yeast regeneration. The removal efficiency of the raw *S. cerevisiae* decreased after being kept for 3–8 months. Storage and reusability investigations confirmed the highest operational stability of immobilized *S. cerevisiae* for eight cycles with retained activity up to 90%.

The findings of this examination indicate that the column technique using the immobilized *S. cerevisiae* leads to obtaining the biosorbent that is easy to handle, excellent, stable for months, sustainable, eco-friendly, and can be applied in food industrial effluent treatment.

**Author Contributions:** Conceptualization, L.A.I., M.E.E.-S., E.E.E., M.H., M.Z., E.S.M. and M.A.-H.; methodology, L.A.I., M.E.E.-S. and E.E.E.; software, L.A.I., M.E.E.-S. and E.E.E.; validation, L.A.I., M.E.E.-S., E.E.E., M.H., M.Z. and M.A.-H.; formal analysis, L.A.I., M.E.E.-S. and E.E.E.; investigation, L.A.I., M.E.E.-S., E.E.E., M.H., M.Z. and M.H.; resources, L.A.I., M.E.E.-S., E.E.E., M.H., M.Z. and M.H.; data curation, L.A.I., M.E.E.-S. and E.E.E.; writing—original draft preparation, L.A.I.; writing—review and editing, L.A.I., M.E.E.-S., E.E.E., M.H., M.Z., E.S.M. and M.A.-H.; visualization, L.A.I. and E.E.E.; supervision, L.A.I., M.E.E.-S., M.Z. and M.A.-H.; project administration, L.A.I., M.Z., M.H., E.S.M. and M.A.-H. All authors have read and agreed to the published version of the manuscript.

**Funding:** This research received no external funding.

**Data Availability Statement:** Not available.

**Acknowledgments:** The authors wish to express their thanks to the directors of the Water Management Research Institute (WMRI), and the Central Laboratory for Environmental Quality Monitoring (CLEQM) at the National Water Research Center (NWRC), Egypt, for their assistance. This work was supported by the Slovak Research and Development Agency under the Contract no. APVV-20-0281. This work was supported by project HUSKROUA/1901/8.1/0072 REVITAL.

**Conflicts of Interest:** The authors declare no conflict of interest.

## References

1. Barrutia, O.; Garbisu, C.; Hernández-Allica, J.; García-Plazaola, J.I.; Becerril, J.M. Differences in EDTA-assisted metal phytoextraction between metallicolous and non-metallicolous accessions of *Rumex acetosa* L. *Environ. Pollut.* **2010**, *158*, 1710–1715. [[CrossRef](#)] [[PubMed](#)]
2. Brunet, J.; Varrault, G.; Zuily-Fodil, Y.; Repellin, A. Accumulation of lead in the roots of grass pea (*Lathyrus sativus* L.), plants trigger systemic variation in gene expression in the shoots. *Chemosphere* **2009**, *77*, 1113–1120. [[CrossRef](#)] [[PubMed](#)]
3. Atkovska, K.; Lisichkov, K.; Ruseska, G.; Dimitrov, A.T.; Grozdanov, A. Removal of heavy metal ions from wastewater using conventional and nanosorbents: A review. *J. Chem. Technol. Metall.* **2018**, *53*, 202–219.
4. Burakov, A.E.; Galunin, E.V.; Burakova, I.V.; Kucherova, A.E.; Agarwal, S.; Tkachev, A.G.; Gupta, V.K. Adsorption of heavy metals on conventional and nanostructured materials for wastewater treatment purposes: A review. *Ecotoxicol. Environ. Saf.* **2018**, *148*, 702–712. [[CrossRef](#)] [[PubMed](#)]
5. Pei, W.; Zhang, J.; Tong, H.; Ding, M.; Shi, F.; Wang, R.; Huo, Y.; Li, H. Removal and reutilization of metal ions on ZIF-67/GO membrane via synergistic photocatalytic-photothermal route. *Appl. Catal. B* **2021**, *282*, 119575. [[CrossRef](#)]
6. Le, V.G.; Vo, D.V.N.; Tran, H.T.; Dat, N.D.; Luu, S.D.N.; Rahman, M.M.; Huang, Y.H.; Vu, C.T. Recovery of Magnesium from Industrial Effluent and Its Implication on Carbon Capture and Storage. *ACS Sustain. Chem. Eng.* **2021**, *9*, 6732–6740. [[CrossRef](#)]
7. Fu, W.; Ji, G.; Chen, H.; Yang, S.; Guo, B.; Yang, H.; Huang, Z. Molybdenum sulphide modified chelating resin for toxic metal adsorption from acid mine wastewater. *Sep. Purif. Technol.* **2020**, *251*, 117407. [[CrossRef](#)]
8. Ezugbe, O.; Rathilal, S. Membrane Technologies in Wastewater Treatment: A Review. *Membranes* **2020**, *10*, 89. [[CrossRef](#)]
9. de Morais Nepel, T.C.; Landers, R.; Vieira, M.G.A.; de Almeida Neto, A.F. Metallic copper removal optimization from real wastewater using pulsed electrodeposition. *J. Hazard. Mater.* **2020**, *384*, 121416. [[CrossRef](#)]
10. Chen, Z.; Wei, W.; Zou, W.; Li, J.; Zheng, R.; Wei, W.; Jie Ni, B.; Chen, H. Integrating electrodeposition with electrolysis for closed-loop resource utilization of battery industrial wastewater. *Green Chem.* **2022**, *8*, 3208–3217. [[CrossRef](#)]
11. Ong, D.C.; de Luna, M.D.G.; Pingul-Ong, S.M.B.; Kan, C.C. Manganese and Iron Recovery from Groundwater Treatment Sludge by Reductive Acid Leaching and Hydroxide Precipitation. *J. Environ. Manag.* **2018**, *223*, 723–730. [[CrossRef](#)] [[PubMed](#)]
12. ElBastamy, E.; Ibrahim, L.A.; Ghandour, A.; Zelenakova, M.; Vranayova, Z.; Abu-Hashim, M. Efficiency of Natural Clay Mineral Adsorbent Filtration Systems in Wastewater Treatment for Potential Irrigation Purposes. *Sustainability* **2021**, *13*, 5738. [[CrossRef](#)]
13. Abdelfattah, I.; Ismail, A.A.; Sayed, F.A.; Almedolab, A.; Aboelghait, K.M. Biosorption of heavy metals ions in real industrial wastewater using peanut husk as efficient and cost-effective adsorbent. *Environ. Nanotechnol. Monit. Manag.* **2016**, *6*, 176–183. [[CrossRef](#)]
14. Tsai, W.C.; De Luna, M.D.G.; Bermillo-Arriegas, H.L.P.; Futralan, C.M.; Colades, J.I.; Wan, M.W. Competitive Fixed-Bed Adsorption of Pb(II), Cu(II), and Ni(II) from Aqueous Solution Using Chitosan-Coated Bentonite. *Int. J. Polym. Sci.* **2016**, *2016*, 1608939. [[CrossRef](#)]
15. Ibrahim, L.A.; El Gammal, H.A.A.; Mahran, B.N. In Vitro, Appraisal and abatement of drainage wastewater pollution in light of utilizing fly ash. *Nat. Sci.* **2017**, *15*, 2017.
16. De Castro, M.L.F.A.; Abad, M.L.B.; Sumalinog, D.A.G.; Abarca, R.R.M.; Paoprasert, P.; de Luna, M.D.G. Adsorption of Methylene Blue Dye and Cu(II) Ions on EDTA-Modified Bentonite: Isotherm, Kinetic and Thermodynamic Studies. *Sustain. Environ. Res.* **2018**, *28*, 197–205. [[CrossRef](#)]
17. Ibrahim, L.A.; Asaad, A.A.; Khalifa, E.A. Laboratory approach for wastewater treatment utilizing chemical addition case study: El-Rahway Drain, Egypt. *Life Sci. J.* **2019**, *16*, 56–67.
18. Ibrahim, L.A.; Elsayed, E.E. Seawater Reinforces Synthesis of Mesoporous and Microporous Zeolites from Egyptian Fly Ash for Removal Ions of Cadmium, Iron, Nickel, and Lead from Artificially Contaminated Water. *Egypt. J. Chem.* **2021**, *64*, 3801–3816. [[CrossRef](#)]
19. Tumampos, S.B.; Ensano, B.M.B.; Pingul-Ong, S.M.B.; Ong, D.C.; Kan, C.C.; Yee, J.J.; de Luna, M.D.G. Isotherm, Kinetics and Thermodynamics of Cu(II) and Pb(II) Adsorption on Groundwater Treatment Sludge-Derived Manganese Dioxide for Wastewater Treatment Applications. *Int. J. Environ. Res. Public Health* **2021**, *18*, 3050. [[CrossRef](#)]
20. Chen, Z.; Wei, W.; Ni, B.-J.; Chen, H. Plastic wastes derived carbon materials for green energy and sustainable environmental applications. *Environ. Funct. Mater.* **2022**, *1*, 34–48. [[CrossRef](#)]
21. Fu, W.; Huang, Z. Magnetic dithiocarbamate functionalized reduced graphene oxide for the removal of Cu(II), Cd(II), Pb(II), and Hg(II) ions from aqueous solution: Synthesis, adsorption, and regeneration. *Chemosphere* **2018**, *209*, 449–456. [[CrossRef](#)] [[PubMed](#)]
22. Cheng, S.Y.; Show, P.L.; Lau, B.F.; Chang, J.S.; Ling, T.C. New Prospects for Modified Algae in Heavy Metal Adsorption. *Trends Biotechnol.* **2019**, *37*, 1255–1268. [[CrossRef](#)] [[PubMed](#)]
23. Thirunavukkarasu, A.; Nithya, R.; Sivashankar, R. Continuous fixed-bed biosorption process: A review. *Chem. Eng. J. Adv.* **2021**, *8*, 1–13. [[CrossRef](#)]
24. Saravanan, A.; Kumar, P.S.; Yaashikaa, P.R.; Karishma, S.; Jeevanantham, S.; Swetha, S. Mixed biosorbent of agro waste and bacterial biomass for the separation of Pb(II) ions from water system. *Chemosphere* **2021**, *277*, 130236. [[CrossRef](#)] [[PubMed](#)]
25. El-Sayed, S.; Hyun-Seog, R.; Subhabrata, D.; Moonis, A.K.; Abou-Shanab, R.A.I.; Chang, S.W.; Jeon, B.H. Algae as a green technology for heavy metals removal from various wastewater. *World J. Microbiol. Biotechnol.* **2019**, *35*, 75–94.
26. Andreu, C.; Ildel Olmo, M. Yeast arming systems: Pros and cons of different protein anchors and other elements required for display. *Appl. Microbiol. Biotechnol.* **2018**, *102*, 2543–2561. [[CrossRef](#)]

27. Negm, N.A.; Abd El Wahed, M.G.; Hassan, A.R.A.; Abou Kana, T.H.A. Feasibility of metal adsorption using brown algae and fungi: Effect of biosorbents structure on adsorption isotherm and kinetics. *J. Mol. Liq.* **2018**, *264*, 292–305. [[CrossRef](#)]
28. Farhan, S.N.; Khadom, A.A. Biosorption of heavy metals from aqueous solutions by *Saccharomyces cerevisiae*. *Int. J. Ind. Chem.* **2015**, *6*, 119–130. [[CrossRef](#)]
29. Savastru, E.; Bulgariu, D.; Zamfir, C.I.; Bulgariu, L. Application of *Saccharomyces cerevisiae* in the Biosorption of Co(II), Zn(II) and Cu(II) Ions from Aqueous Media. *Water* **2022**, *14*, 976. [[CrossRef](#)]
30. Malairuang, K.; Krajang, M.; Sukna, J.; Rattanapradit, K.; Chamsart, S. High Cell Density Cultivation of *Saccharomyces cerevisiae* with Intensive Multiple Sequential Batches Together with a Novel Technique of Fed-Batch at Cell Level (FBC). *Processes* **2020**, *8*, 1321. [[CrossRef](#)]
31. Zhu, W.L.; Yang, H.; He, C.; Yang, J.; Yu, X.; Wu, G.; Zeng, S.; Tarre, M. Green, Preparation, performances and mechanisms of magnetic *Saccharomyces cerevisiae* bionanocomposites for atrazine removal. *Chemosphere* **2018**, *200*, 380–387. [[CrossRef](#)] [[PubMed](#)]
32. Farbo, M.G.; Urgeghe, P.P.; Fiori, S.; Marceddu, S.; Jaoua, S.; Migheli, Q. Adsorption of ochratoxin A from grape juice by yeast cells immobilised in calcium alginate beads. *Int. J. Food Microbiol.* **2016**, *217*, 29–34. [[CrossRef](#)] [[PubMed](#)]
33. Özer, A.; Özer, D. Comparative study of the biosorption of Pb(II), Ni(II) and Cr(VI) ions onto *S. cerevisiae*: Determination of biosorption heats. *J. Hazard. Mater.* **2003**, *100*, 219–229. [[CrossRef](#)] [[PubMed](#)]
34. Mirmahdia, R.S.; Mofida, V.; Zoghib, A.; Daranib, K.K.; Mortazavian, A.M. Risk of low stability *Saccharomyces cerevisiae* ATCC 9763-heavy metals complex in gastrointestinal simulated conditions. *Heliyon* **2022**, *8*, e09452. [[CrossRef](#)] [[PubMed](#)]
35. Massoud, R.; Khosravi-Darani, K.; Sharifan, A.; Asadi, G.H.; Younesi, H. The Biosorption Capacity of *Saccharomyces Cerevisiae* for Cadmium in Milk. *Dairy* **2020**, *1*, 169–176. [[CrossRef](#)]
36. Wang, J.; Chen, C. Biosorption of heavy metals by *Saccharomyces cerevisiae*: A review. *Biotechnol. Adv.* **2006**, *24*, 427–451. [[CrossRef](#)]
37. Marques, P.; Pinheiro, H.M.; Rosa, M.F. Cd(II) removal from aqueous solution by immobilised waste brewery yeast in fixed-bed and airlift reactors. *Desalination* **2007**, *214*, 343–351. [[CrossRef](#)]
38. Machado, M.D.; Soares, E.V.; Soares, H.M.V.M. Selective recovery of copper, nickel and zinc from ashes produced from *Saccharomyces cerevisiae* contaminated biomass used in the treatment of real electroplating effluents. *J. Hazard. Mater.* **2010**, *184*, 357–363. [[CrossRef](#)]
39. Machado, M.D.; Soares, E.V.; Soares, H.M.V.M. Removal of heavy metals using a brewer's yeast strain of *Saccharomyces cerevisiae*: Chemical speciation as a tool in the prediction and improving of treatment efficiency of real electroplating effluents. *J. Hazard. Mater.* **2010**, *180*, 347–353. [[CrossRef](#)]
40. Fu, F.; Wang, Q. Removal of heavy metal ions from wastewaters: A review. *J. Environ. Manag.* **2011**, *92*, 407–418. [[CrossRef](#)]
41. Jiang, W.; Xu, Y.; Li, C.; Lv, X.; Wang, D. Biosorption of cadmium(II) from aqueous solution by chitosan encapsulated *Zygosaccharomyces rouxii*. *Environ. Prog. Sustain. Energy* **2013**, *32*, 1101–1110. [[CrossRef](#)]
42. Amirnia, S.; Ray, M.B.; Margaritis, A. Heavy metals removal from aqueous solutions using *Saccharomyces cerevisiae* in a novel continuous bioreactor-biosorption system. *Chem. Eng. J.* **2015**, *264*, 863–872. [[CrossRef](#)]
43. De Rossi, A.; Rigueto, C.V.T.; Dettmer, A.; Colla, L.M.; Piccin, J.S. Synthesis, characterization, and application of *Saccharomyces cerevisiae*/alginate composites beads for adsorption of heavy metals. *J. Environ. Chem. Eng.* **2020**, *8*, 104009. [[CrossRef](#)]
44. De Rossi, M.R.; Rigon, M.; Zapparoli, R.D.; Braidò, L.M.; Colla, G.L.; Dotto, J.S.; Piccin, J.S. Chromium (VI) biosorption by *Saccharomyces cerevisiae* subjected to chemical and thermal treatments. *Environ. Sci. Pollut. Res.* **2018**, *25*, 19179–19186. [[CrossRef](#)] [[PubMed](#)]
45. Rusu, L.; Grigoraş, C.G.; Simion, A.I.; Suceveanu, E.M.; Şuteu, D.; Harja, M. Application of *Saccharomyces cerevisiae*/Calcium Alginate Composite Beads for Cephalexin Antibiotic Biosorption from Aqueous Solutions. *Materials* **2021**, *14*, 4728. [[CrossRef](#)]
46. Lee, S.B.; Choi, W.S.; Jo, H.J.; Yeo, S.-H.; Park, H.-D. Optimization of air-blast drying process for manufacturing *Saccharomyces cerevisiae* and non-*Saccharomyces* yeast as industrial wine starters. *AMB Express* **2016**, *6*, 105. [[CrossRef](#)]
47. Göksungur, Y.; Üren, S.; Güvenç, U. Biosorption of cadmium and lead ions by ethanol treated waste baker's yeast biomass. *Bioresour. Technol.* **2005**, *96*, 103–109. [[CrossRef](#)]
48. El-Sayed, M.T. Removal of Lead(II) by *Saccharomyces cerevisiae* AUMC 3875. *Ann. Microbiol.* **2016**, *63*, 1459–1470. [[CrossRef](#)]
49. Araujo, L.G.; de Borba, T.R.; de Ferreira, R.V.; de P. Canevesi, R.L.S.; Silva, E.A.; da Dellamano, J.C.; Marumo, J.T. Use of calcium alginate beads and *Saccharomyces cerevisiae* for biosorption of 241Am. *J. Environ. Radioact.* **2020**, *223–224*, 106399. [[CrossRef](#)]
50. Moreno Rivas, S.C.; Armenta Corral, R.I.; Frascuillo Félix, M.D.C.; Islas Rubio, A.R.; Vázquez Moreno, L.; Ramos-Clamont Montfort, G. Removal of Cadmium from Aqueous Solutions by *Saccharomyces cerevisiae*—Alginate System. *Materials* **2019**, *12*, 4128. [[CrossRef](#)]
51. Elgarhy, A.H.; Mahran, B.N.A.; Liu, G.; Salem, T.A.; ElSayed, E.E.; Ibrahim, L.A. Comparative study for removal of phosphorus from aqueous solution by natural and activated bentonite. *Sci. Rep.* **2022**, *12*, 19433. [[CrossRef](#)] [[PubMed](#)]
52. Clesceri, L.S.; Rice, E.W.; Baird, R.B.; Eaton, A.D. (Eds.) *Standard Methods for the Examination of Water and Wastewater*, 23rd ed.; American Public Health Association (APHA), American Water Works Association (AWWA) and Water Environment Federation (WEF): Washington DC, USA, 2017.
53. Das, N.; Vimala, R.; Karthika, P. Biosorption of heavy metals—An overview. *Indian J. Biotechnol.* **2008**, *7*, 159–169.

54. Zinicovscaia, I.; Grozdov, D.; Yushin, N.; Abdusamadzoda, D.; Gundorin, S.; Rodlovskaya, E.; Kristavchuk, O. Metal removal from chromium containing synthetic effluents by *Saccharomyces cerevisiae*. *Desalin. Water Treat.* **2000**, *178*, 254–270. [[CrossRef](#)]
55. Martins, R.J.E.; Vilar, V.J.P.; Boaventura, R.A.R. Kinetic Modelling of Cadmium and Lead Removal by Aquatic Mosses. *Braz. J. Chem. Eng.* **2014**, *31*, 229–242.
56. Xiong, Y.; Xu, J.; Shan, W.; Lou, Z.; Fang, D.; Zang, S.; Han, G. A new approach for rhenium(VII) recovery by using modified brown algae *Laminaria japonica* adsorbent. *Bioresour. Technol.* **2013**, *127*, 464–472. [[CrossRef](#)] [[PubMed](#)]
57. Dada, A.O.; Olalekan, A.P.; Olatunya, A.M.; Dada, O. Langmuir, Freundlich, Temkin and Dubinin–Radushkevich isotherms studies of equilibrium sorption of Zn<sup>2+</sup> onto phosphoric acid modified rice husk. *IOSR J. Appl. Chem.* **2012**, *3*, 38–45.
58. Oves, M.; Khan, M.S.; Zaidi, A. Biosorption of heavy metals by *Bacillus thuringiensis* strain OSM29 originating from industrial effluent contaminated north Indian soil. *Saudi Sci. J. Biol. Sci.* **2013**, *20*, 121–129. [[CrossRef](#)]
59. Say, R. Biosorption of cadmium(II), lead(II) and copper(II) with the filamentous fungus *Phanerochaete chrysosporium*. *Bioresour. Technol.* **2001**, *76*, 67–70. [[CrossRef](#)] [[PubMed](#)]
60. Dutta, A.; Zhou, L.; Castillo-Araiza, C.O.; De Herdt, E. Cadmium(II), Lead(II), and Copper(II) Biosorption on Baker’s Yeast (*Saccharomyces cerevisiae*). *J. Environ. Eng.* **2016**, *142*, C6015002. [[CrossRef](#)]
61. Guler, U.A.; Ersan, M. *S. cerevisiae* cells modified with nZVI: A novel magnetic biosorbent for nickel removal from aqueous solutions. *Desalin. Water Treat.* **2015**, *23*, 1–13.
62. Guler, U.A.; Sarioglu, M. Mono and binary component biosorption of Cu(II), Ni(II), and methylene blue onto raw and pretreated, *S. cerevisiae*: Equilibrium and kinetics. *Desalin. Water Treat.* **2014**, *52*, 4871–4888. [[CrossRef](#)]
63. Asgari, G.; Roshani, B.; Ghanizadeh, G. The investigation of kinetic and isotherm of fluoride adsorption onto functionalize pumice stone. *J. Hazard. Mater.* **2012**, *17*, 123–132. [[CrossRef](#)] [[PubMed](#)]
64. Gialamouidis, D.; Mitrakas, M.; Liakopoulou-Kyriakides, M. Equilibrium, thermodynamic and kinetic studies on biosorption of Mn(II) from aqueous solution by *Pseudomonas* sp., *Staphylococcus xylosus* and *Blakeslea trispora* cells. *J. Hazard. Mater.* **2010**, *182*, 672–680. [[CrossRef](#)] [[PubMed](#)]
65. Stathatou, P.M.; Athanasiou, C.E.; Tsezos, M.; Goss, J.W.; Blackburn, L.C.; Turlomousis, F.; Mershin, A.; Sheldon, B.W.; Padture, N.P.; Darling, E.M.; et al. Lead removal at trace concentrations from water by inactive yeast cells. *Commun. Earth Environ.* **2022**, *3*, 132. [[CrossRef](#)]
66. El-Naggar, N.E.A.; Hamouda, R.A.; Mousa, I.E.; Abdel-Hamid, M.S.; Rabei, N.H. Statistical optimization for cadmium removal using *Ulva fasciata* biomass: Characterization, immobilization and application for almost-complete cadmium removal from aqueous solutions. *Sci. Rep.* **2018**, *8*, 12456. [[CrossRef](#)]
67. Sundararaju, S.; Manjula, A.; Kumaravel, V.; Muneeswaran, T.; Vennila, T. Biosorption of nickel ions using fungal biomass *Penicillium* sp. MRF1 for the treatment of nickel electroplating industrial effluent. *Biomass. Convers. Biorefinery* **2022**, *12*, 1059–1068. [[CrossRef](#)]
68. Xu, P.; Liu, L.; Zeng, G.; Huang, D.; Lai, C.; Zhao, M.; Huang, C.; Li, N.; Wei, Z.; Wu, H.; et al. Heavy metal-induced glutathione accumulation and its role in heavy metal detoxification in *Phanerochaete chrysosporium*. *Appl. Microbiol. Biotechnol.* **2014**, *98*, 6409–6418. [[CrossRef](#)]
69. Zhang, S.; Zang, X.; Chang, C.; Yuanm, Z.; Wang, T.; Zhao, Y.; Yang, X.; Zhang, Y.; La, G.; Wu, K.; et al. Improvement of tolerance to lead by filamentous fungus *Pleurotus ostreatus* HAU-2 and its oxidative responses. *Chemosphere* **2016**, *150*, 33–39. [[CrossRef](#)] [[PubMed](#)]
70. Zhao, Y.; Gu, X.; Gao, S.; Geng, J.; Wang, X. Adsorption of tetracycline (TC) onto montmorillonite: Cations and humic acid effects. *Geoderma* **2012**, *183*, 12–18. [[CrossRef](#)]
71. Bahafid, W.; Joutey, N.T.; Sayel, H.; Iraqui-Houssaini, M.; El Ghachtouli, N. Chromium adsorption by three yeast strains isolated from sediments in Morocco. *Geomicrobiol. J.* **2013**, *30*, 422–429. [[CrossRef](#)]
72. Cabras, P.; Meloni, M.; Pirisi, F.M.; Farris, G.A.; Fatichenti, F. Yeast and pesticide interaction during aerobic fermentation. *Appl. Microbiol. Biotechnol.* **1988**, *29*, 298–301. [[CrossRef](#)]